

Thermal Expansion of Liquid Helium II[†]

R. F. Harris-Lowe and K. A. Smee

Department of Physics, Royal Military College, Kingston, Ontario, Canada

(Received 16 December 1969)

The thermal-expansion coefficient of liquid helium II under its saturated vapor pressure has been measured from 0.85 K to within 0.4 mK of the λ transition. The capacitive technique employed was well suited for these measurements. With the aid of the Clausius-Mossotti equation, we could resolve a relative change in density of 1 part in 10^6 in a manner free from sources of systematic error. The data below 1.60 K were analyzed to obtain information about the density derivatives of the Landau parameters Δ , p_0 , and μ with the following results:

$$\frac{\rho}{\Delta} \frac{\partial \Delta}{\partial \rho} = -0.763 \pm 0.012 \quad \text{and} \quad \frac{1}{2} \frac{\rho}{\mu} \frac{\partial \mu}{\partial \rho} + 2 \frac{\rho}{p_0} \frac{\partial p_0}{\partial \rho} + \frac{\rho}{\Delta} \frac{\partial \Delta}{\partial \rho} = -1.638 \pm 0.077.$$

The results of a reanalysis of the data obtained by other workers in this temperature interval are presented in order to provide a valid comparison with the present results. The techniques employed also allowed measurements to be taken to within 0.4 mK of the λ transition. At this temperature, the uncertainty in an individual measurement (one standard deviation) had reached about $\pm 10\%$. This represents a considerable improvement over previous measurements and allows a detailed examination of the validity of the Pippard-Buckingham-Fairbank relations. It was found that the agreement between theory and experiment is good if the temperature dependence of all the terms in these relations is taken into account. The capacitance bridge was also employed to measure absolute values of the dielectric constant of liquid helium at temperatures of approximately 1.0 K and a frequency of 5 kHz. Analysis of these measurements yielded a value for the molar polarizability of $0.123\,296 \pm 0.000\,030 \text{ cm}^3 \text{ mole}^{-1}$.

I. INTRODUCTION

The thermal-expansion coefficient of liquid helium II under its saturated vapor pressure

$$\alpha_s = -\frac{1}{\rho} \left(\frac{\partial \rho}{\partial T} \right)_s$$

has been the subject of several investigations in recent years.¹⁻⁴ Although it should be possible to make precise measurements of α_s , the disagreement between the results is larger than can be explained by the quoted experimental errors. This paper will describe measurements of the expansion coefficient by a capacitive technique from a temperature of 0.85 K to 0.4 mK below the λ transition and it is believed that the results can be employed to resolve the above discrepancies. The results below 2.0 K have been briefly reported previously.⁵

The measurements presented here will be discussed in two sections; one covering the low-temperature region below 2.0 K, and the other the λ -transition region. In the former, Landau's theory^{6,7} of liquid helium II is applicable and the measurements can be used to obtain information concerning the density derivatives of the Landau parameters Δ , p_0 , and μ . At temperatures close to the λ point the theory of phase transitions is applicable and it has been customary to analyze results in terms of the relations of Pippard^{8,9} and of Buckingham and Fairbank.¹⁰ These relations

will be referred to as the PBF relations.

II. EXPERIMENTAL METHOD

A. Capacitance Measurements

The dielectric constant of liquid helium can be related to its density by the Clausius-Mossotti equation

$$\frac{K_e - 1}{K_e + 2} = \frac{4\pi\alpha_M}{3M} \rho, \quad (1)$$

where M is the molecular weight of helium, ρ is the liquid density, K_e is the dielectric constant, and α_M is the molar polarizability. An analysis by Edwards² indicates that the molar polarizability remains strictly constant from room temperature down to, and throughout, the liquid-helium temperature region. It follows that for any capacitor with a liquid-helium dielectric, a change in capacitance δC can be related to a change in density $\delta\rho$ by the equation

$$\frac{\delta\rho}{\rho} = \frac{1}{3} \left(\frac{3}{4\pi\alpha_M} + \frac{2}{V_M} \right) \left(V_M - \frac{4\pi\alpha_M}{3} \right) \frac{\delta C}{C} \quad (2)$$

if the physical dimensions of the capacitor are fixed. V_M is the molar volume of the helium. Thus the observation of small changes in capacitance with temperature of a cell immersed in liquid helium under its saturated vapor pressure can be used to find the expansion coefficient α_s . In these experiments the molar polarizability α_M was

assumed to be $0.1233 \text{ cm}^3/\text{mole}$, which was a compromise between the value of $0.1232 \text{ cm}^3/\text{mole}$ determined by Chase *et al.*⁴ and the value of 0.12355 ± 0.0002 resulting from the measurements of Edwards² corrected to the experimental frequency of 5 kHz used in this research. A measurement of the dielectric constant and molar polarizability (described in Sec. V) confirmed this value. Appropriate values for the molar volume were taken from Kerr and Taylor,³ although only a very small error would be introduced by treating this term as a constant.

The capacitance-change measurements were accomplished with a General Radio 1615-A capacitance bridge operated in conjunction with a Princeton Applied Research JB-6 lock-in amplifier. Reference 11 describes the technique employed for the measurements below 2.0 K. However, after some measurements had been taken in the region close to the λ point we found it desirable to attempt to improve the resolution. Consequently some minor changes were incorporated in the interconnection of the bridge and detection circuits which resulted in the desired improvement in the signal-to-noise ratio and in the resolution of capacitance changes. Figure 1 is a block diagram of the modified electronics and Fig. 2 illustrates a typical sequence of capacitance-change measurements. As can be seen, each measurement consisted of an alternating set of capacitance determinations at two temperatures. Then a three-parameter linear least-squares fit to these data provided a value for both the capacitance change between these temperatures and its uncertainty (one standard deviation). With this measurement technique and method of analysis we successfully canceled out the effect of

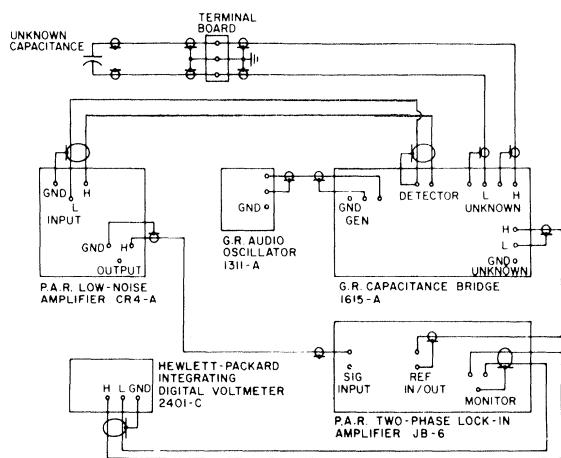


FIG. 1. Block diagram showing interconnection of GR 1615-A capacitance bridge and detection circuits.

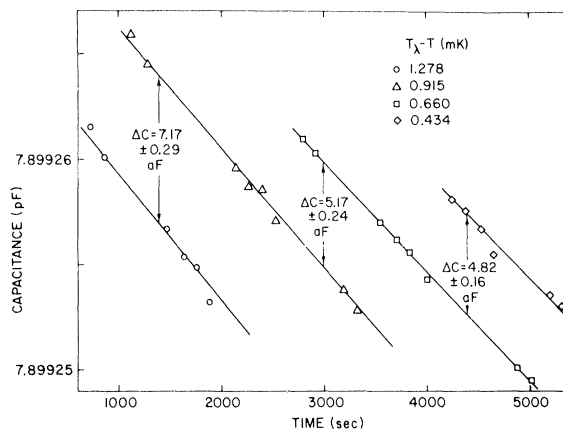


FIG. 2. Sequence of capacitance measurements at four different temperatures in the region of the λ transition.

the slow constant drift in capacitance apparent in Fig. 2. This drift was probably due to a slow change in the ambient temperature of the bridge. As can be seen from the figure, the method is capable of resolving relative changes in capacitance of at least 4 parts in 10^8 , and absolute changes of 0.4 aF.

B. Experimental Cell

A schematic drawing of the experimental cell is shown in Fig. 3. Basically it consists of a shielded parallel-plate capacitor with an area of 6.4 cm^2 and a plate spacing of approximately 0.7 mm. The employment of a three-terminal capacitance measurement technique completely eliminates the effects of stray capacitances to ground. As a result of this and the cell design, the problems involved in correcting for dead capacitances due to dielectric supports, or for variations in the capacitances of the coaxial leads, were eliminated. In addition, the design, which included a spring-loading feature (not shown in Fig. 3) to counteract the effects of relative contraction between brass and Teflon, minimized the thermal contraction of the capacitor dimensions. Calculations based on the measured total change in cell capacitance between room and liquid-helium temperatures showed that any such changes had negligible effect in the temperature range of interest.

Care was taken in the construction of the cell and in the experimental procedures to ensure that the helium which entered the capacitor gap between the pressed surfaces of the brass spacer and the outer brass case was free from impurities. Standard precautions ensured that there were no impurities present prior to any run, but the possibility cannot be ruled out that there were some impurities present in the liquid helium transferred

into the glass Dewar. However there was never any visible evidence of such impurities, and the restricted entrance into the capacitor gap should have prevented the entrance of such particles if present. On one occasion the Dewar was sealed off immediately after the liquid helium was exhausted and the cryostat was then allowed to warm to room temperature. Even employing the assumption that the resultant pressure in the Dewar was due solely to air which had been present as solid-impurity particles in the liquid helium, we estimated that the relative error in measurements due to impurities on that occasion was less than 3 parts in 10^7 . Consequently, it can be reasonably assumed that any errors due to impurities were negligible.

It can be seen from Fig. 3 that because the experimental cell is below the helium bath level, the pressure exerted on the helium between the capacitor plates was higher than the vapor pressure by an amount given by a pressure head of helium which varied between 5 and 15 cms. Thus the expansion coefficient was not measured at the vapor pressure but at a slightly higher pressure. However, the data of Elwell and Meyer¹² show that the resultant change in the expansion coefficient can be neglected. In addition, as the density is dependent on pressure as well as temperature, any changes in the bath level during the measurement could result in an error because of a resultant change in density. The pressure head falls continuously throughout a run, but the method of analysis employed to obtain capacitance differences eliminates any such continuous change in the density (or continuous drift in the electronics). In any event, even without cancellation the effect is small compared to other sources of experimental error.

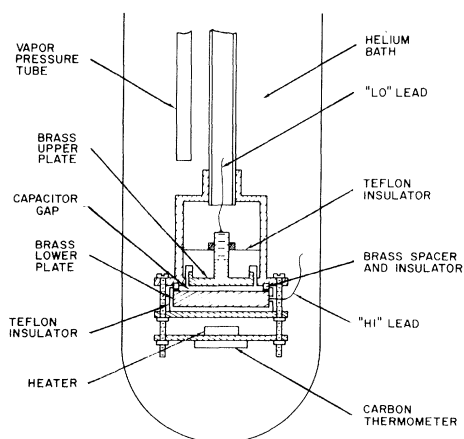


FIG. 3. Schematic drawing of apparatus showing the parallel-plate capacitance cell and thermometry arrangements.

Finally, if the cell is not at the bottom of the bath any change in the density when the temperature is changed will result in a change in the pressure head of the bath, with an additional effect on the density. Again, calculations show that this effect is entirely negligible with respect to other sources of experimental uncertainty.

C. Thermometry

Temperatures were determined by calibrating a carbon resistance thermometer against the 1958 ^4He vapor-pressure scale of temperatures.¹³ The resistance was measured with a Cryotronics Inc. ML-155AC resistance bridge operated at 155 Hz. Temperatures were controlled by adjusting the pumping speed of an Edwards High Vacuum Ltd. 18B-3 vapor booster pump backed by a Kinney vacuum KDH-130 rotary pump, in conjunction with a Cryotronic ML-1300A temperature controller and 100- Ω helium bath heater. The performance of the bridge was improved by the use of a Hewlett-Packard 419A dc null voltmeter which monitored the bridge off-balance voltage. It was found that temperatures could be easily held constant to within 10 μK during any measurement.

In the temperature interval 0.85–2.00 K, a 10- Ω , $\frac{1}{2}$ -W Allen-Bradley carbon resistor with the insulating coating removed was used. The thermometer power level ranged between 0.15×10^{-8} and 2.5×10^{-8} W, depending upon the temperature. In this temperature interval, vapor pressures were measured with a Consolidated Vacuum Corporation GM 100A McLeod gauge and a Wallace and Tiernan FA-135 mercury manometer. Because of the diameter of the vapor-pressure tube (0.2185 cm), corrections for the thermomolecular pressure difference were applied at the lowest temperatures.¹⁴ The carbon thermometer was calibrated by a least-squares fit of the data to both the three-constant formula of Clement and Quinell,¹⁵ and the $\log_{10}(R)$ -versus- $\log_{10}(P)$ formula of Cunsolo *et al.*¹⁶ Although there was no significant difference in the answers provided by these two techniques, we calculated temperatures with the calibration obtained by the latter method because it was found that the constants were stable from run to run within experimental error. The constants obtained by the former method appeared to be highly sensitive to very small changes in the input data.

When measurements were started in the λ -transition region it was found necessary to improve the sensitivity of the carbon thermometer. This was done by replacing the 10- Ω resistor with four 27- Ω $\frac{1}{2}$ -W Allen-Bradley resistors connected in series. The insulating coating was removed and the resistors were then encapsulated in an epoxy

resin (Stycast 2850 FT with catalyst 24 LV). This coating was added in order to prevent any unknown resistance changes due to the penetration of helium into the carbon. It had been found that the value of the resistance at the λ point (R_λ) increased steadily with time during a run. It was thought that this was perhaps due to a slow penetration of helium but the encapsulation had no noticeable effect on the drift, whose origin remains puzzling. However, the coating did ensure that there were no sharp changes in the internal self-heating of the resistor at the λ point. The thermometer power level was 1.8×10^{-8} W per resistor.

R_λ was found by monitoring the change in resistance with time as the helium bath was allowed to warm slowly through the transition. Figure 4 is a chart recording of a typical warming curve and illustrates how R_λ could be determined to within 0.1Ω . The steady increases of R_λ with time caused a serious experimental difficulty at temperatures within 20 mK of T_λ , but this problem was resolved by a method suggested by Tyson.¹⁷ It was noted that the rate of drift decreased with time. Consequently, measurements were started only after some 20 h had elapsed after a helium transfer. Figure 5 shows the subsequent variation of R_λ with time during one of the runs. It was assumed that resistances corresponding to other temperatures in the region of the transition were drifting by the same amount. For calibration purposes all the resistances measured at various times throughout the run were then corrected to a common time (the last determination of R_λ).

In the λ -transition region vapor pressures were measured with a Texas Instruments Model 144-01 fused-quartz pressure gauge with a range from 0

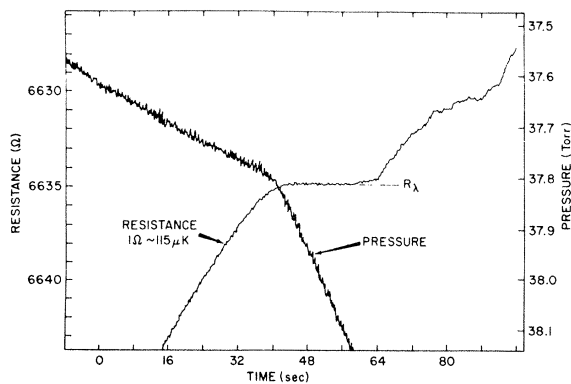


FIG. 4. Variation of vapor pressure and resistance as the helium bath warms through T_λ . The plateau in the resistance curve determines R_λ , the value of resistance at T_λ .

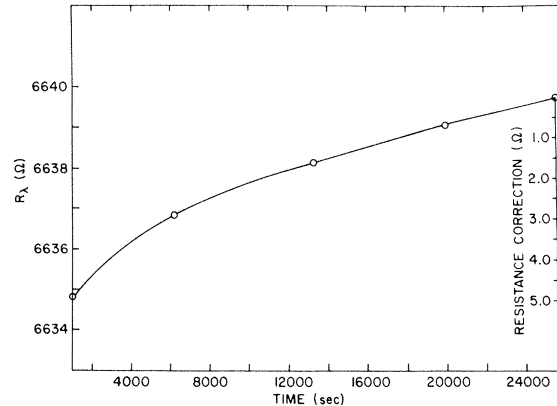


FIG. 5. Thermometry drift. Observed time dependence of R_λ during a typical experiment. The ordinate on the right gives the resistance correction applied for calibration purposes.

to 300 Torr. With this instrument, pressures could be determined to within 0.01 Torr, providing excellent calibration data for the thermometer. Pressures were converted to temperatures as before,¹³ and together with the corresponding drift-corrected resistance values, were fitted by least-squares to the three-constant Clement and Quinell formula.¹⁵ This was used because in the region close to the λ transition the temperature changes became very small making it more convenient to employ a calibration which converted resistance directly into temperature. The standard deviation of the residuals between calibrated and measured temperatures was 0.053 mK, a value which is nicely accounted for by the precision of the vapor-pressure measurements. The transition temperature T_λ for each run was taken to be the calibrated temperature corresponding to the appropriate value of R_λ , as found from a short extrapolation of the calibration curve. Values obtained in this way were above the accepted value of 2.172 K by an amount which varied from 0.021 to 0.133 mK. The precision and accuracy with which vapor-pressure measurements could be taken gave us another check on the experimental location of the λ transition. Figure 4, which showed the resistance change through the transition, also illustrates the concurrent vapor-pressure variation. As can be seen, there is a sharp break in the slope of the pressure curve which occurred at a pressure of 37.81 Torr, and which corresponded in time to the start of the resistance plateau which indicated the value of R_λ .

As a consequence of the cell design and thermometry arrangements we did not take any measurements at temperatures above T_λ . It was considered that the possibility of temperature inhomogeneity

genities in the bath precluded accurate temperature determinations.

III. EXPERIMENTAL RESULTS

A. Low-Temperature Region (0.85 to 2.00 K)

Figure 6 illustrates the results for α_s as a function of temperature below 2.0 K, with the different symbols indicating measurements taken on different dates. Temperature increments were approximately 50 mK. Also included on the figure are the results of Atkins and Edwards¹ and Kerr and Taylor.³ It can be seen that the scatter of individual measurements from the smooth curve drawn through the results is satisfactorily accounted for by the error bars shown on one point of the inset, representing one standard deviation as determined directly from the capacitance-difference measurements. If we assume that the conversion of a change in capacitance to a change in density by Eq. (2) introduces no errors, then the ultimate accuracy of the measurements, as limited by possible systematic errors in measurement, is estimated to be $\pm 2\%$. This figure combines the 96% confidence limits which can be placed on the calibration of the lowest bridge decades and an estimated systematic error of $\pm 1\%$ arising from the temperature measurements.

The coefficient of expansion at the saturated vapor pressure α_s is related to that at constant pressure (α_P) by the relation

$$\alpha_s = \alpha_P - \left(\frac{\partial P}{\partial T}\right)_s \left[\frac{1}{\rho u_1^2} \left(1 + \frac{T u_1^2 \alpha_P^2}{c_P} \right) \right], \quad (3)$$

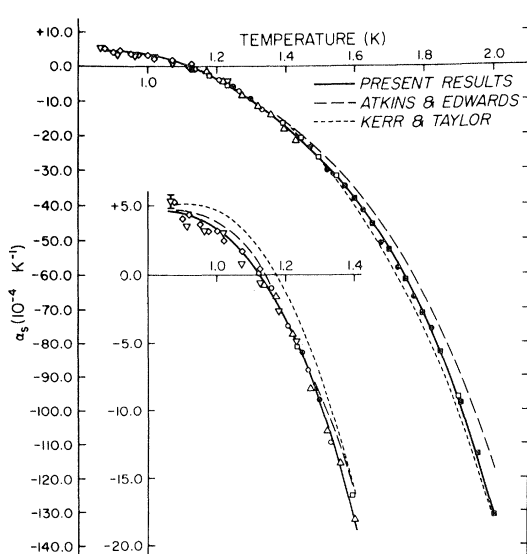


FIG. 6. Coefficient of thermal expansion at saturated vapor pressure below 2.0 K. Atkins and Edwards (Ref. 1); Kerr and Taylor (Ref. 3).

TABLE I. Smoothed values for the coefficient of thermal expansion at the saturated vapor pressure (α_s) and at constant pressure (α_P) between 0.85 and 2.15 K.

Temperature (K)	α_s (10^{-4} K^{-1})	α_P (10^{-4} K^{-1})	Temperature (K)	α_s (10^{-4} K^{-1})	α_P (10^{-4} K^{-1})
0.85	+ 4.6	+ 4.7	1.55	- 32.2	- 28.7
0.90	+ 4.5	+ 4.6	1.60	- 38.0	- 33.9
0.95	+ 4.0	+ 4.1	1.65	- 44.6	- 39.7
1.00	+ 3.3	+ 3.4	1.70	- 52.2	- 46.5
1.05	+ 2.2	+ 2.5	1.75	- 61.2	- 54.7
1.10	+ 0.8	+ 1.2	1.80	- 71.3	- 63.8
1.15	- 1.0	- 0.5	1.85	- 83.2	- 74.6
1.20	- 3.2	- 2.5	1.90	- 97.6	- 87.7
1.25	- 6.0	- 5.1	1.95	- 113.0	- 101.9
1.30	- 9.5	- 8.3	2.00	- 129.6	- 117.2
1.35	- 13.6	- 12.0	2.05	- 150.0	- 136.1
1.40	- 18.0	- 16.1	2.10	- 189.6	- 174.1
1.45	- 22.0	- 19.6	2.15	- 263.4	- 246.2
1.50	- 26.8	- 23.9			

where u_1 is the velocity of first sound,¹⁸ $(\partial P/\partial T)_s$ is the slope of the vapor-pressure curve,¹³ and c_P is the specific heat of liquid helium at constant pressure.^{19,20} Table I lists graphically smoothed values for α_s and α_P at various temperatures.

B. λ -Transition Region

The experimental results for α_s in the region of the λ transition are shown in Fig. 7. Once again the different symbols refer to measurements taken during different runs, and the error bars indicate one standard deviation as determined directly from the capacitance-difference measurements. There is a large variation in the size of the error bars in the region within 10 mK of T_λ . In general, those points with the smaller error bars were obtained last. For these measurements the temperature increments were always chosen to be less than $0.4(T_\lambda - \bar{T})$, where \bar{T} is the mean of the two temperatures. A simple calculation shows that this choice ensures that the error due to the finite size of the temperature difference is less than $\frac{1}{2}\%$ for these results. As for the lower-temperature results, the ultimate accuracy of these measurements is estimated to be $\pm 2\%$.

The solid line of Fig. 7 represents an equation of the form

$$\alpha_s = A \log_{10}(T_\lambda - T) + B, \quad (4)$$

where the parameters have the values $A = (143.5 \pm 2.4) \times 10^{-4} \text{ K}^{-1}$ and $B = (-25.5 \pm 3.2) \times 10^{-4} \text{ K}^{-1}$, and together with the error limits of one standard deviation have been determined by a weighted, linear, least-squares fit to the data within 100 mK of T_λ . The weights were taken to be the inverse of the variance of each point as determined from

the capacitance difference measurements. As can be seen, this equation provides a good representation of the data in the above temperature interval. However, it should be emphasized that although the expansion coefficient at constant pressure α_p (and consequently α_s) is expected to become a linear function of $\log_{10}(T_\lambda - T)$ near the transition, the asymptotic region for this behavior should not occur until within approximately 5 mK of the transition (as will be shown in Sec. IV). Consequently, the parameters for this equation, as determined from this experiment, should not be employed to evaluate the parameters appearing in asymptotic forms of the theory.

C. Other Results

As mentioned previously, α_s has been investigated by a number of other workers, and the results of Atkins and Edwards¹ and Kerr and Taylor³ below 2.0 K have already been shown on Fig. 6. The results of these authors and others^{2,4} in the transition region are displayed on Fig. 8. It can be seen that although all workers have observed a linear relationship in this region there is considerable disagreement between some of the results. The tabulated values of Table II lead to the conclusion that the present results are in good agreement with the results of Atkins and Edwards¹ and Edwards,² but are considerably different from those obtained by Kerr and Taylor³ or Chase *et al.*⁴ The disagreement with the results quoted by Kerr and Taylor can be understood when it is realized that their experiment consisted of volumetric measurements which were fitted to analytical expressions derived from theory and experience, and that these expressions for the molar volume were

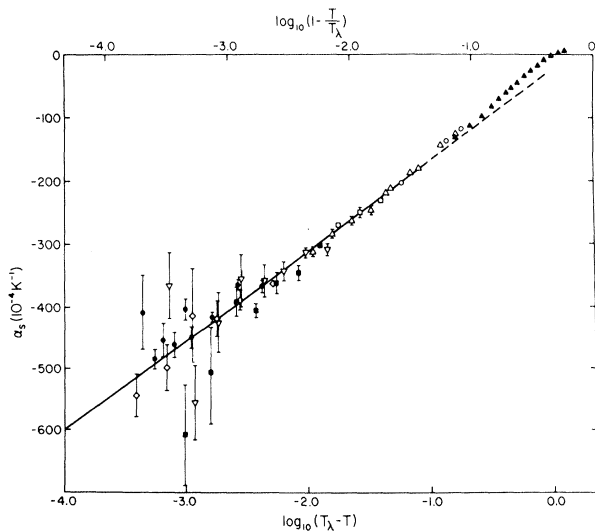


FIG. 7. Coefficient of thermal expansion at saturated vapor pressure in the region of T_λ .

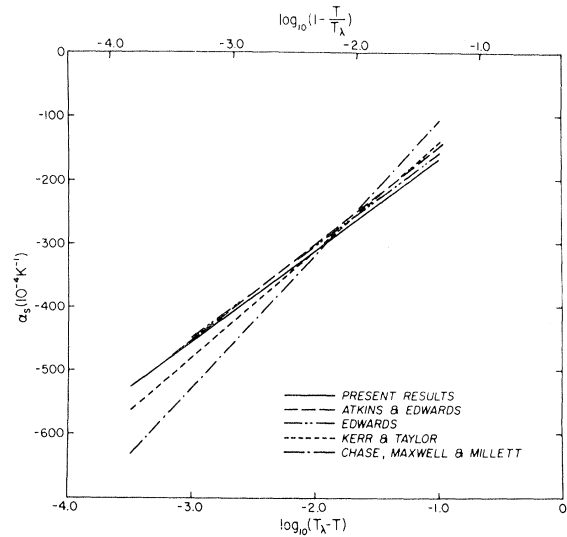


FIG. 8. A comparison of various measurements of the coefficient of thermal expansion in the region of the λ transition (Refs. 1-4).

then differentiated to give the expansion coefficient. With the average relative volume deviation quoted as 6×10^{-5} , it would be unreasonable to expect the measurements to give anything but a rough estimate of the expansion coefficient at temperatures below 1.35 K or at temperatures within 5 mK of the transition, because in these temperature intervals such a scatter is larger than the predicted change in relative volume with a reasonable temperature increment. The disagreement with the results of Chase *et al.* is partially resolved when error bars appropriate to their quoted values of scatter in capacitance measurements are added to their curve.

IV. ANALYSIS

A. Low-Temperature Region

According to Landau,^{6,7} the entropy of liquid helium may be written as the sum of contributions

TABLE II. Values for the parameters A and B of Eq. (4) in the transition region. [$\alpha_s = A \log_{10}(T_\lambda - T) + B$].

	$10^4 A$	$10^4 B$
Present results	143.5 ± 2.4	-25.5 ± 3.2
Atkins and Edwards (Ref. 1) ^a	152.7	3.2
Edwards (Ref. 2)	145.0	-15.0
Kerr and Taylor (Ref. 3)	168.4	24.7
Chase <i>et al.</i> (Ref. 4)	210.0	100.0

^aThe results listed for Atkins and Edwards were obtained by a least-squares fit to their smoothed data for α_s within 100 mK of T_λ .

from the phonon and roton portions of its excitation spectrum. This conclusion also applies to the coefficient of expansion α_P . Atkins and Edwards¹ have developed the expression

$$\left(-\frac{\alpha_r u_1^2}{s_r}\right) = a + b \left[\frac{\Delta}{kT} \left(1 + \frac{\frac{3}{2}(kT/\Delta)^2}{1 + 3kT/2\Delta} \right) \right], \quad (5)$$

$$\text{where } a = \frac{1}{2} \frac{\rho}{\mu} \frac{\partial \mu}{\partial \rho} + 2 \frac{\rho}{p_0} \frac{\partial p_0}{\partial \rho} + \frac{\rho}{\Delta} \frac{\partial \Delta}{\partial \rho} - 1$$

$$\text{and } b = -\frac{\rho}{\Delta} \frac{\partial \Delta}{\partial \rho}.$$

In the above, Δ , p_0 , and μ are the Landau parameters, k is the Boltzmann constant, u_1 is the velocity of first sound, and s_r and α_r are the roton contributions to the entropy and expansion coefficient, respectively. We would expect this equation to be theoretically valid only at temperatures below about 1.6 K. This is because at higher temperatures the neutron scattering data of Yarnell *et al.*²¹ indicate that the Landau parameter Δ is temperature dependent whereas the statistical-mechanical theory employed in the derivation of Eq. (5) implicitly assumes that these parameters are independent of temperature.

Figure 9 is a plot of our results expressed in terms of Eq. (5), where the ordinate Y is given by the term on the left-hand side of the equation, and the abscissa X is given by the term in square brackets on the right. Δ/k was assumed to have the constant value 8.65 K, in agreement with the measurements of Yarnell *et al.*²¹ at 1.1 K. Values for α_r and s_r were obtained by subtracting the phonon contributions

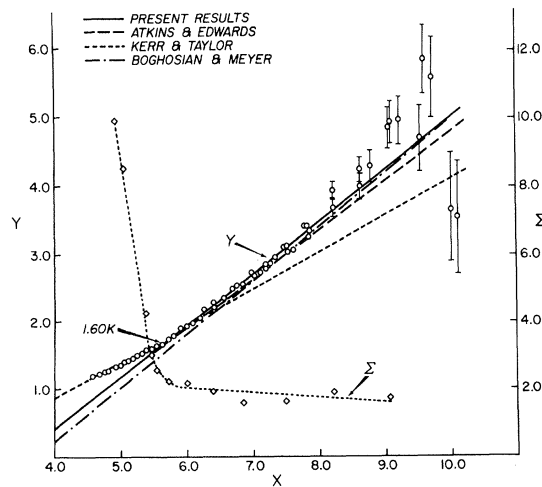


FIG. 9. Representation of expansion-coefficient data below 2.0 K in terms of Eq. (5). $Y = -\alpha_r u_1^2 / s_r$ and

$$X = \frac{\Delta}{kT} \left[1 + \frac{\frac{3}{2}(kT/\Delta)^2}{1 + 3kT/2\Delta} \right].$$

Lower temperatures are to the right.

$$\alpha_{ph} = \frac{16\pi^5 k^4 T^3}{15h^3 c^3} \left(\frac{1}{c} \frac{\partial c}{\partial P} + \frac{1}{3} K_T \right), \quad (6)$$

$$s_{ph} = 16\pi^5 k^4 T^3 / 45h^3 c^3 \rho, \quad (7)$$

from the measured values of α_P and the total entropy.^{19,20} In the above expressions, h is Planck's constant, K_T is the isothermal compressibility [given by the term in square brackets in Eq. (3)], and c is the velocity of phonons. The values for the latter and its pressure derivative $\partial c / \partial P$ were obtained from Mills [Ref. 22, Eq. (5)].

Once again the error bars represent one standard deviation as determined from the capacitance difference measurements. An analysis of the data indicates that it is consistent with a linear relationship between the variables X and Y at temperatures below 1.60 K (to the right in Fig. 9). That this is so can be seen by observing the behavior of the parameter Σ which is also plotted on Fig. 9, and which is defined by the equation

$$\Sigma(X) = \frac{1}{N_X - 2} \sum_{i=1}^{N_X} \frac{(\delta Y_i)^2}{\sigma_{Y_i}^2}, \quad (8)$$

where the summation is taken over the N_X data points which satisfy the relation $X_i \geq X$. Here δY_i is the residual of the i th datum point as determined from a weighted, linear, least-squares fit to the above N_X points and $\sigma_{Y_i}^2$ is the variance of the variable Y_i as determined from the capacitance-difference measurements (and, of course, is the inverse of the weight for this variable). Ideally, if the data were consistent with a straight line, and if all sources of experimental error were reflected in the weights chosen for each point, then the parameter Σ would have a value of unity. However, there are other sources of experimental error, such as an error in temperature measurement. These would not add to the scatter in a capacitance-difference measurement and thus would not be reflected in the weights chosen for our data points. Consequently, even if the data points were selected from a region which satisfied a linear hypothesis we would expect that the corresponding value of Σ should be a constant somewhat larger than unity. With these considerations in mind, the behavior of the parameter as displayed on Fig. 9 indicates that the data are consistent with a linear relation only for $X \geq 5.6$, or correspondingly, for temperatures less than 1.60 K. The least-squares fit for the data in this range results in values of $a = -2.638 \pm 0.077$ and $b = 0.763 \pm 0.012$ for the parameters of Eq. (5). The error limits correspond to one standard deviation. These values are slightly different from those quoted previously⁵ because the temperature interval selected as the linear region has been changed slightly as a consequence of the above test to establish the consistency of a linear fit.

In order to provide a meaningful comparison with the results of other authors, their results between 0.9 and 1.60 K have been reanalyzed in the above manner to give appropriate values for the parameters a and b and, in addition, a value for the temperature at which $\alpha_P = 0$. Thus their results, as displayed in Fig. 9 and Table III, are not necessarily the results quoted by these authors but instead have been modified by this new analysis. The change in the results quoted for Atkins and Edwards¹ is largely due to the fact that they employed the entropy data of Hercus and Wilks,²³ which are about 10% higher than the entropy data^{19,20} employed for our analysis. The change in the results quoted for Kerr and Taylor³ is a consequence of employing only their smoothed results below 1.6 K. Once again, any differences between Table III and the earlier results quoted in Ref. 5 are a consequence of the different temperature interval selected for analysis. There appears to be satisfactory agreement between the present results and those of Atkins and Edwards¹ and Boghosian and Meyer²⁴ (whose values for α_P at $P=0$ were obtained by extrapolation from measurements at higher pressures).

B. λ -Transition Region

It has been customary to analyze measurements of the expansion coefficient in terms of the PBF relation

$$\left(\frac{\alpha_P}{\rho}\right) = \left(\frac{\partial T}{\partial P}\right)_\lambda \frac{c_P}{T} - \left(\frac{\partial s}{\partial P}\right)_t, \quad (9)$$

where $t = T_\lambda(P) - T$

and $T_\lambda(P)$ is the λ temperature at pressure P . Although this equation is a rigorous thermodynamic relation at any point *not* on the transition line, it has often been misinterpreted by treating the term $(\partial s/\partial P)_t$ either as a constant or as a slowly varying function of t which necessarily approaches the value $(\partial s/\partial P)_\lambda$ as $t \rightarrow 0$. However, as Ahlers has

TABLE III. Tabulated values obtained from expansion-coefficient data below 2.00 K. Values for parameters a and b obtained by least-squares fit of data to Eq. (5), as described in text.

	a	$b =$ $\frac{\rho}{\Delta} \frac{\partial \Delta}{\partial \rho}$	$\alpha + b + 1 =$ $\frac{1}{2\mu} \frac{\partial \mu}{\partial \rho} + 2 \frac{\rho}{p_0} \frac{\partial p_0}{\partial \rho}$	$T_{\alpha_P=0}$ (K)
Present results	-2.64 ±0.08	0.76 ±0.01	-0.88 ±0.06	1.138 ±0.01
Atkins and Edwards (Ref. 1)	-2.47	0.73	-0.74	1.150
Kerr and Taylor (Ref. 3)	-1.31	0.54	+0.23	1.185
Boghosian and Meyer Ref. 24)	-2.96	0.79	-1.17	1.144

pointed out,²⁵ the transition line is characterized as a line of discontinuous derivatives in the P - T plane, and consequently there is no immediate mathematical necessity for either of the above assumptions to be true. The same comments hold true, of course, for the last term in the second PBF relation

$$\frac{K_T}{\rho} = \left(\frac{\partial T}{\partial P}\right)_\lambda \frac{\alpha_P}{\rho} - \left(\frac{\partial v}{\partial P}\right)_t. \quad (10)$$

These same assumptions have been employed by Buckingham and Fairbank¹⁰ to try to show that the specific heat at constant volume approaches a finite value at the transition. Recently, Wheeler and Griffiths²⁶ have shown by rigorous stability arguments that c_v "will in general be finite, or at least not divergent along a continuous curve." A similar argument can be used to show that the same conclusion holds for the terms $(\partial v/\partial P)_t$ and $(\partial s/\partial P)_t$. Consider the integral equation

$$\int_{P_1, t}^{P_2, t} \left(\frac{\partial s}{\partial P}\right)_t dP = s(P_2, t) - s(P_1, t). \quad (11)$$

Since the entropy is considered to be continuous at all points, even on the transition line, then the integral of $(\partial s/\partial P)_t$ along a line of constant t must have a finite value as the transition line is approached. A similar statement can of course be made for $(\partial v/\partial P)_t$, and it can be concluded that these derivatives do not diverge everywhere along the transition line. However, these considerations do not rule out the occurrence of integrable divergencies in these terms at isolated points on the transition line, such as at the lower λ point. Although there is no apparent reason for any point to be different from any other point on the transition line, it has been noted²⁷ that the behavior of the line near the lower λ point is qualitatively different from the behavior near the upper λ point. Experimental evidence appears to indicate that the terms $(\partial s/\partial P)_t$ and $(\partial v/\partial P)_t$ are continuous and nondivergent as the transition line is approached, but even so, the first-sound velocity measurements of Barmatz and Rudnick²⁸ near the transition indicate that the temperature dependence of these terms is not negligible, at least to within a few mK of the transition. Thus an analysis of expansion coefficient measurements in terms of the PBF relations which treats these derivatives as constant must be viewed with some reservations unless only those measurements taken within the above indicated asymptotic region have been included.

Ahlers²⁵ has recently reanalyzed the results of Barmatz and Rudnick,²⁸ correcting for the temperature variations of the PBF "constants." He shows that if the specific heat along a given isobar can be written

$$c_p = A + B \ln t, \quad (12)$$

$$\text{then } \left(\frac{\partial s}{\partial P} \right)_t = \left(\frac{\partial s}{\partial P} \right)_\lambda + \Delta_p^s, \quad (13)$$

$$\text{where } \Delta_p^s = \frac{1}{T_\lambda} \left[\frac{dB}{dP} - \frac{dA}{dP} - \frac{1}{T_\lambda} \left(\frac{\partial T}{\partial P} \right)_\lambda (B - A) \right] t \\ - \frac{1}{T_\lambda} \left[\frac{dB}{dP} - \frac{1}{T_\lambda} \left(\frac{\partial T}{\partial P} \right)_\lambda B \right] t \ln t.$$

Thus this assumption about the specific heat implies a singular temperature-dependent contribution Δ_p^s to the derivative $(\partial s/\partial P)_t$. Although the term Δ_p^s vanishes at the transition, analysis shows that it makes an appreciable contribution to the expansion coefficient at temperatures more than a few mK below the transition and must be accounted for in any analysis.

The term Δ_p^s was not evaluated directly from Eq. (13) because of the lack of information about the pressure derivatives of the parameters A and B . However, the term can be evaluated by integrating Ahlers's specific-heat data²⁵ along suitable paths in the He II region to give values for the entropy as a function of the parameter t at two different pressures. The entropy at given t and the vapor pressure was estimated from a simple integration of c_p/T at the saturated vapor pressure. The value of the entropy at a higher pressure and given t was obtained by integrating Ahlers's data for $c_v(t')/T$ along a path of constant volume (26.80 cc mole⁻¹) from the transition line to a suitable value of the parameter $t' = T_{\lambda v} - T$, where $T_{\lambda v}$ is the transition temperature corresponding to the above molar volume. The relation between t' and t can be determined from a knowledge of the derivative $(\partial P/\partial T)_v$ in the region of interest. This was obtained from the paper by Elwell and Meyer¹² along with Kierstead's measurements of density and pressure along the transition line.²⁹ These results were also employed to obtain a value for the higher pressure. Once expressions for the entropy have been obtained in the above manner a simple division by the pressure difference provides an expression for the term $(\partial s/\partial P)_t$ which has the same form as Eq. (13), and which can be used to provide numerical estimates for the term Δ_p^s as a function of t when Ahlers's²⁵ value $(\partial s/\partial P)_\lambda = -0.911 \text{ cm}^3 \text{ mole}^{-1} \text{ K}^{-1}$ is subtracted.

So far, the discussion has been concerned with the relationship between α_p and c_p along the line of constant pressure which meets the lower λ point, whereas the available measurements are α_s and c_s along the saturated vapor-pressure curve. However, it is easy to show that the relation

$$\left(\frac{\alpha_s}{\rho} \right) = \left(\frac{\partial T}{\partial P} \right)_\lambda \frac{c_s}{T} - \left(\frac{\partial s}{\partial P} \right)_t + \left(\frac{\partial P}{\partial T} \right)_s \left(\frac{\partial v}{\partial P} \right)_t \quad (14)$$

holds along the latter curve. The last term in the above equation is also a function of t as the transition is approached, but the term is small ($\sim 5\%$) compared to $(\partial s/\partial P)_t$ and its temperature dependence is not significant with respect to Eq. (14). Values for $(\partial P/\partial T)_s$ were obtained from Ref. 13, and the term $(\partial v/\partial P)_t$ was calculated in the manner described by Ahlers.²⁵ If, in addition, it is assumed that the correction term Δ_p^s has substantially the same value on the vapor-pressure curve as it has on the line of constant pressure which meets the lower λ point, then it is possible to employ Eq. (14) to predict α_s/ρ as a function of c_s/T .

Figure 10 is a plot of the present results for α_s/ρ plotted in the manner suggested by Eq. (14). The solid line on the figure represents the predicted curve given by this equation, where values for the various terms on the right have been calculated in the manner just described. Of course Eq. (14) does require a knowledge of c_s/T as a function of t . This information was obtained from the specific-heat data of Hill and Lounasmaa²⁰ and Kellers, Buckingham, and Fairbank.^{10,30,31} The latter's results were employed in the region within 20 mK of the transition. The dashed curve of

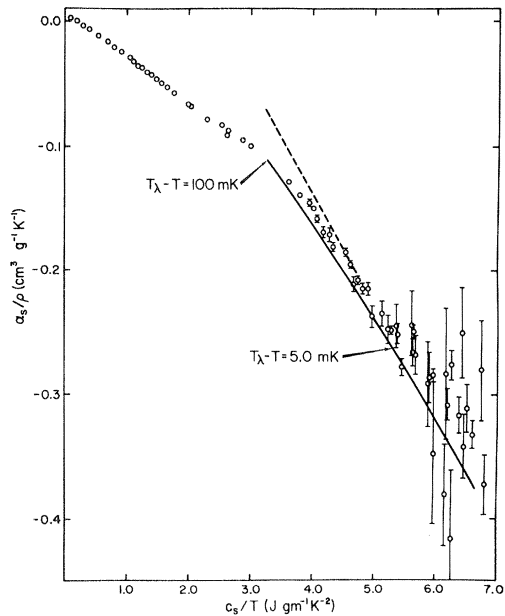


FIG. 10. Representation of expansion-coefficient data in the transition region in terms of Eq. (14). Note both experimental and theoretical results refer to α_s and c_s , whereas earlier treatments have compared the experimental results for α_s to a theory which is calculated in terms of α_p . Solid line is calculated curve with $(\partial s/\partial P)_t$ evaluated by Eq. (13); dashed line is calculated asymptotic curve with

$$\left(\frac{\partial s}{\partial P} \right)_t = \left(\frac{\partial s}{\partial P} \right)_\lambda = -0.911 \text{ cm}^3 \text{ mole}^{-1} \text{ K}^{-1}.$$

Fig. 10 represents the asymptotic curve predicted by Eq. (14) when $(\partial s/\partial P)_t$ is treated as a constant equal to $(\partial s/\partial P)_\lambda$, and thus corresponds to the standard predictions based on the PBF equations as modified to account for the fact that measurements were taken at the saturated vapor pressure.

It can be seen that the agreement between theory and experiment is very good, especially when it is considered that a small change in the theoretical calculations such as the employment of Ahlers's value for the slope of the λ line³² instead of Kierstead's value²⁹ would have effectively removed any discrepancies between the solid theoretical curve and the experimental results. However, this fact does not justify such a substitution because it is an unfortunate feature of the theoretical calculations that they involve the cancellation of rather large terms to result in small final values, and the discrepancies could result from small errors in parameters other than $(\partial P/\partial T)_\lambda$. Nevertheless, the results and calculations depicted on Fig. 10 illustrate clearly that the experimental results follow the trend of the predicted solid curve of the present theory in the temperature interval between 5 and 100 mK. Thus we can conclude that any analysis of expansion-coefficient measurements in terms of the asymptotic form of the PBF relations (dashed curve) must be incorrect unless only those results in the temperature interval where the two theories overlap are included. From Fig. 10 it is apparent that the asymptotic region where the dashed and solid curves become indistinguishable falls within 5 mK of the transition.

V. DIELECTRIC CONSTANT

As mentioned previously, the apparatus could be used to take absolute measurements of the dielectric constant of liquid helium. The method consisted simply of observing the change in capacitance as the helium bath level dropped below the capacitance cell. Since it is the ratio of two capacitances that is important in this measurement, the absolute calibration of the capacitance bridge is not critical but the internal calibration has to be carefully adjusted. The calibration techniques described earlier allow these to be set accurately to within 1 part in 10^5 without difficulty.

A major advantage of this technique over previous absolute capacitance measurements⁴ is that the two capacitance determinations are taken at the same temperature by a three-terminal technique, and no corrections are required for either dead capacitance due to supports or capacitance to

TABLE IV. Experimental values of the dielectric constant and molar polarizability at 5 kHz.

Temperature (K)	K_ϵ	α_M (cm ³ mole ⁻¹)
1.072	1.057 248 $\pm 0.000 020$	0.123 319 $\pm 0.000 040$
1.018	1.057 233 $\pm 0.000 010$	0.123 284 $\pm 0.000 020$
Combined		0.123 296 $\pm 0.000 030$

ground or for thermal-contraction effects. There are, however, two possible corrections: one due to the helium vapor remaining within the cell, and the other due to the helium film remaining on the surfaces of the capacitance cell after the disappearance of the main bulk of the helium. Calculations show that the error resulting from any residual vapor at low temperatures is entirely negligible with respect to other sources of error, and a reasonable estimate of the thickness of the helium film results in a correction to the measurements which is about the same magnitude as the quoted experimental errors. The results of two separate measurements taken on different dates are given in Table IV. The value for the molar polarizability was calculated with the aid of Eq. (1) and the density data of Kerr and Taylor.³ The error limits quoted in Table IV are based on an estimate of the maximum possible errors in the capacitance ratio determination; the limits for the second measurement are smaller because of an improvement in the bridge calibration.

In spite of the high accuracies which have resulted from the employment of this technique it has to be remembered that the purity of the helium sample in this experiment could not be absolutely guaranteed. However, the earlier discussion indicated that it could be reasonably assumed that any impurities had negligible effect and the agreement both between the two measurements, and between these measurements and the results of Edwards² ($\alpha_M = 0.123 55 \pm 0.0002$ cm³/mole at 5 kHz) and Chase *et al.*⁴ ($\alpha_M = 0.1232$ cm³/mole), support this conclusion.

ACKNOWLEDGMENTS

We would like to thank Dr. M. H. Edwards for many helpful discussions and L. H. Lowther and T. A. J. Keefer for help in the construction of the cryostat.

*Research for this paper was supported by the Defence Research Board of Canada, Grant No. 9510-23.

¹K. R. Atkins and M. H. Edwards, *Phys. Rev.* **97**, 1429 (1955).

- ²M. H. Edwards, *Can. J. Phys.* **36**, 884 (1958).
³E. C. Kerr and R. D. Taylor, *Ann. Phys. (N. Y.)* **26**, 292 (1964).
⁴C. E. Chase, E. Maxwell, and W. E. Millett, *Physica* **27**, 1129 (1961).
⁵R. F. Harris-Lowe and K. A. Smees, *Phys. Letters* **28A**, 246 (1968).
⁶L. Landau, *J. Phys. (U.S.S.R.)* **5**, 71 (1941).
⁷L. Landau, *J. Phys. (U.S.S.R.)* **11**, 91 (1947).
⁸A. B. Pippard, *Phil. Mag.* **1**, 473 (1956).
⁹A. B. Pippard, *Elements of Classical Thermodynamics* (Cambridge U. P., Cambridge, England, 1964), p. 143.
¹⁰M. J. Buckingham and W. M. Fairbank, in *Progress in Low-Temperature Physics*, edited by C. J. Gorter (North-Holland, Amsterdam, 1961), Vol. III, Chap. III.
¹¹R. F. Harris-Lowe and K. A. Smees, *Rev. Sci. Instr.* **40**, 725 (1969).
¹²D. L. Elwell and H. Meyer, *Phys. Rev.* **164**, 245 (1967).
¹³F. G. Brickwedde, H. van Dijk, M. Durieux, J. R. Clement, and J. K. Logan, *J. Res. Natl. Bur. Std. (U. S.)* **64A**, 1 (1960).
¹⁴T. R. Roberts and S. G. Sydorjak, *Phys. Rev.* **102**, 304 (1956).
¹⁵J. R. Clement and E. H. Quinnell, *Rev. Sci. Instr.* **23**, 213 (1952).
¹⁶S. Cunsolo, M. Santini, and M. Vicentini-Missoni, *Cryogenics* **5**, 168 (1965).
¹⁷J. A. Tyson, *Phys. Rev.* **166**, 166 (1967).
¹⁸K. R. Atkins and R. A. Stasior, *Can. J. Phys.* **31**, 1156 (1953).
¹⁹H. C. Kramers, J. D. Wasscher, and C. J. Gorter, *Physica* **18**, 329 (1952).
²⁰R. W. Hill and O. V. Lounasmaa, *Phil. Mag.* **2**, 143 (1957).
²¹J. L. Yarnell, G. P. Arnold, P. J. Bendt, and E. C. Kerr, *Phys. Rev.* **113**, 1379 (1959).
²²R. L. Mills, *Ann. Phys. (N. Y.)* **35**, 410 (1965).
²³G. R. Hercus and J. Wilks, *Phil. Mag.* **45**, 1163 (1954).
²⁴C. Boghosian and H. Meyer, *Phys. Rev.* **152**, 200 (1966).
²⁵G. Ahlers, *Phys. Rev.* **182**, 352 (1969).
²⁶J. C. Wheeler and R. B. Griffiths, *Phys. Rev.* **170**, 249 (1968).
²⁷W. E. Keller, *Helium-3 and Helium-4* (Plenum, New York, 1969), p. 257.
²⁸M. Barmatz and I. Rudnick, *Phys. Rev.* **170**, 224 (1967).
²⁹H. A. Kierstead, *Phys. Rev.* **162**, 153 (1967).
³⁰C. F. Kellers, Ph.D. thesis, Duke University, 1960 (unpublished).
³¹W. M. Fairbank and C. F. Kellers, in *Proceedings of the Conference on Critical Phenomena, Washington, D. C.*, 1965 (U. S. G. P. O., Washington, D. C., 1966).
³²G. Ahlers, *Phys. Rev.* **171**, 275 (1968).

Photon Counting Statistics of Harmonic Signal Mixed with Thermal Light. I. Single Photoelectron Counting*

A. K. Jaiswal and C. L. Mehta

Department of Physics and Astronomy, University of Rochester, Rochester, New York 14627
(Received 10 November 1969)

In this paper, we consider the photoelectron counting distribution when the wave field incident on the detector is a mixture of harmonic signal and thermal noise. An expression for the factorial moment-generating function of the number of counts is obtained in terms of the eigenvalues of an associated integral equation. This expression is then used to evaluate the factorial cumulants of the number of counts. The results are valid for an arbitrary counting interval. The extension to photoelectron counting with several detectors is considered in paper II of the present investigation.

I. INTRODUCTION

The problem of obtaining the statistical properties of a harmonic signal mixed with Gaussian noise has first been considered by Rice.¹ More recently, the problem has received a renewed interest in connection with the photoelectron counting distribution when the light incident on the detector is a mixture of coherent and thermal

(Gaussian) light.²⁻⁷ Several experiments⁸⁻¹⁰ have indicated that the light from a laser working well above threshold may approximately be considered to be a coherent light mixed with a small amount of thermal light. Further, the study of the statistical properties of such a mixed radiation has applications to the determination of the spectral profiles using heterodyne techniques (see, for ex-